International Journal of Applied Power Engineering (IJAPE)
Vol. 15, No. 3, September 2026, pp. 1314~1326
ISSN: 2252-8792, DOI: 10.11591/ijape.v15.i3.pp1314-1326

Design and build charging system tools in hybrid power plants with pico-hydro turbine cross flow and solar panels using buck boost converter based on PID controller

Yulianta Siregar[1], Christian Kevin Imanuel Simarmata[1], Issarachai Ngamroo[2]
[1]Department of Electrical Engineering, Faculty of Engineering, Universitas Sumatera Utara, Medan, Indonesia
[2]Department of Electrical Engineering, School of Engineering, King Mongkut's Institute of Technology Ladkrabang (KMITL), Bangkok, Thailand

Article Info

Article history:

Received Aug 15, 2025
Revised Jun 25, 2026
Accepted Aug 15, 2026

Keywords:

Buck-boost converter
Crossflow water turbine
Hybrid charging system
PID controller
Solar panel

ABSTRACT

Indonesia itself has a potential for water energy of up to 75,091 MW, spread across the country, but its utilization has only reached around 7.2%. In addition, Indonesia's location in the equatorial region provides it with an average of 8-10 hours of solar radiation per day, with a potential solar energy output of 4.80 kWh/m^2/day. However, utilizing two or more new and renewable energy sources poses challenges for synchronising sources from different plants. For this reason, the methodology of this research is to design a charging system for a hybrid power plant, a wind turbine, an air crossflow, and a 50 Wp solar panel on a battery using a non-inverting buck-boost converter, with Arduino Mega2560 as the control logic centre. The PID control parameters were determined through trial and error, with Kp = 0.8, Ki = 0.04, and Kd = 0.002. The voltage is set to 14.4 V, and the hybrid system maintains a stable voltage at 14.263 V with an average error of 1.243%. The system can charge the battery optimally. It is recorded that it takes 3 hours to charge the battery.

Corresponding Author:

Yulianta Siregar
Department of Electrical Engineering, Faculty of Engineering, Universitas Sumatera Utara
Medan, Indonesia
Email: julianta_srg@usu.ac.id

1. INTRODUCTION

Increased use of fossil energy leads to an increase in greenhouse gas emissions, resulting in climate instability as well as an increase in global temperatures and sea levels. Many researchers have proven that emissions contributed the greatest to climate change from 1750 to 2005 CO_2 [1]-[3]. Therefore, the development of new and renewable energy is a top priority in efforts to reduce carbon emissions and maintain sustainable energy availability. Several new and renewable energy sources, such as wind energy [4]-[6], solar cell [7]-[9], hydropower [10]-[13], and geothermal [14], [15], have been the main focus in this endeavor. Indonesia itself has a potential for water energy of up to 75,091 MW spread throughout Indonesia, but its utilization has only reached around 7.2%. Most of this water energy use is for power generation. Hydroelectric power plants have proven to be reliable and account for 66% of the total 7 GW of new and renewable energy power plants, according to Institute for Essential Services Reform in 2019 [15]-[18]. In addition, Indonesia's location in the equatorial region provides this region with an average of 8-10 hours of solar radiation per day, with a potential solar energy that can be produced of 4.80 kWh/m^2/day [19]-[21]. Therefore, a strategy is needed to take advantage of this availability. This is by integrating the two energy sources in a single system, commonly known as a hybrid system. New hybrid and renewable electric energy systems offer a number of advantages that include high reliability, optimal efficiency, and a friendly environment with minimal emissions even without emissions. However, it should be noted that the implementation of a hybrid system requires thorough consideration of various technical aspects. This includes the selection of suitable currents as well as effective distribution strategies to ensure a stable and efficient supply of power to a wide range of loads. In this context, choosing DC current and implementing a buck-boost converter system can be the right solution to deal with these challenges [22], [23].

According to previous research, a battery charging system was modelled using a buck-boost non-inverting converter at solar panels. The system was designed with a minimum input voltage of 18 V and a maximum output voltage of 52 V, with an expected output voltage of 48 V. Software SIMetrix was used to ensure the desired performance. The system is also equipped with driver switching on and off controlled by a PIC16F877 microcontroller, which serves to set the system in buck or boost mode [24]. Then, another previous research topic was a buck converter battery charging controller design for a photovoltaic system. They designed a buck converter by simulating the system using the MATLAB SIMULINK application and the perturb and observe (P&O) algorithm. This P&O algorithm ensures that the system operates at maximum power point, while the buck converter serves to lower the voltage to a certain level. This system uses a PID controller to regulate the battery charging process. The use of a PID controller has been proven to increase the efficiency of the battery charging system by reducing the losses generated [25]. Meanwhile, the lead-acid battery charging system on solar panels has been conducted. This system implements maximum power point tracking (MPPT) with the perturb and observe (P&O) algorithm. This research maintains the state of charge (SoC) battery at 60%, using a buck converter to lower the voltage before charging the battery. Conventional diodes on buck converters were replaced with MOSFETs, which were proven to improve battery charging efficiency compared to conventional buck converters [26].

Based on previous research and the stated problem, the novelty of this research is designing a battery charging system for hybrid power plants using pico-hydro cross flow turbines and solar panels. This system uses a buck-boost converter type non-inverting based on a PID controller to maintain a stable voltage level. Two voltage sources from different plants will be combined; when the DC voltage is already at the same level, the voltage can be parallelised to improve the charging efficiency of the battery.

2. METHOD

This research is planned to be carried out in the Department of Electrical Engineering, Universitas Sumatera Utara, Medan City, Indonesia. The design of the charging system in a hybrid plant uses components related to the charging system. The overall design of a pico hydro power plant using a crossflow turbine and solar panels is shown in Figure 1. The block diagram of the charging system in a hybrid plant is shown in Figure 2. It is described as a block diagram of the system offered. Meanwhile, the charging system schema for a hybrid is shown in Figure 3. The flow diagram is a chart of the design process in the research, which explains the working system of the design as seen in Figure 4.

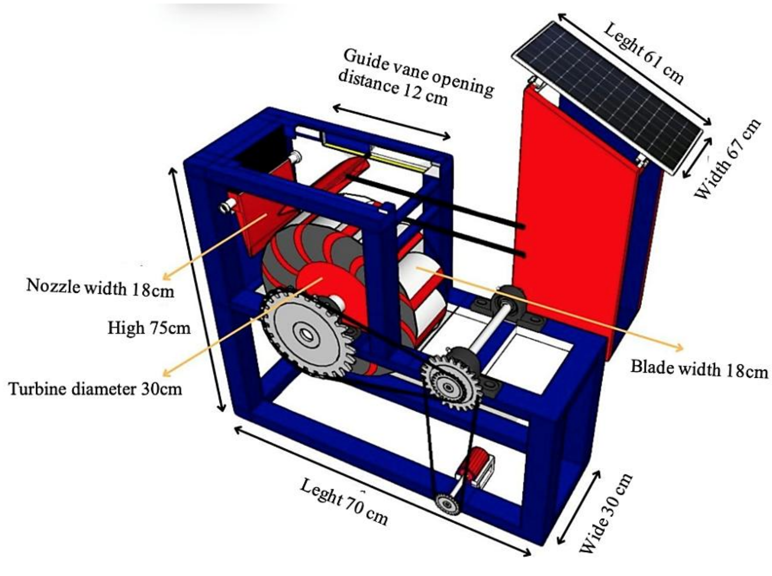

Figure 1. Design of crossflow turbine and solar panel

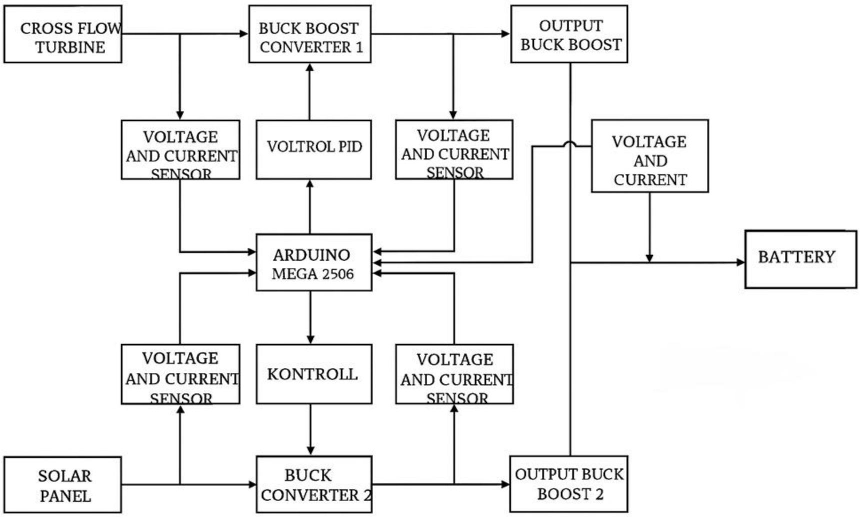

Figure 2. System diagram blocks charging hybrid

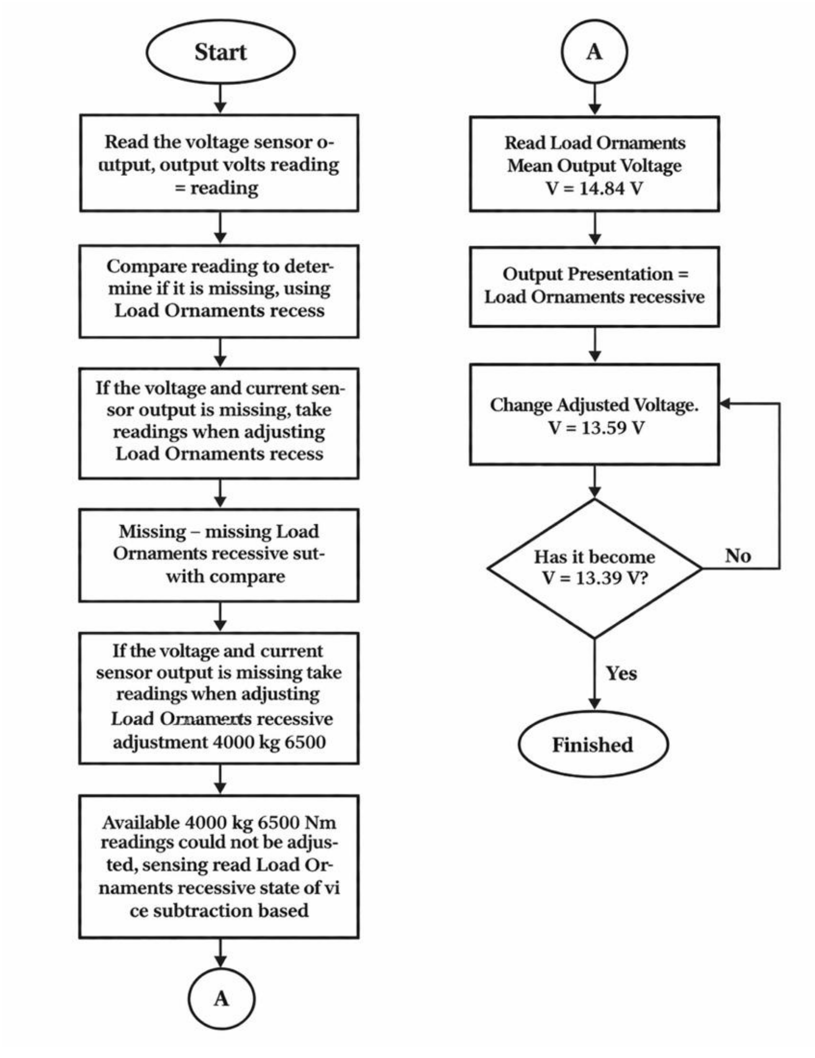

Figure 3. Schema charging system hybrid

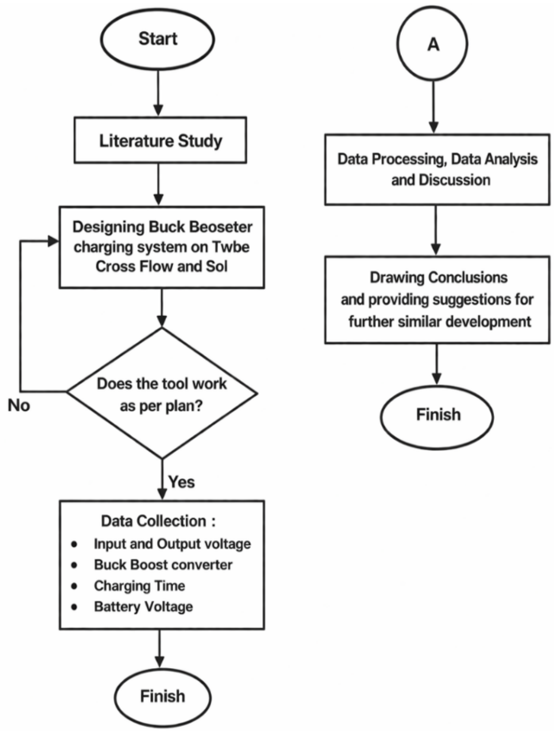

Figure 4. Research flow diagram

This charging system design uses a non-inverting buck boost converter system, which is one type of buck-boost converter that has been explained in the previous chapter. This design requires several components, such as resistors, capacitors, diodes, MOSFETs, inductors, and others. In this system, the MOSFET driver will be controlled using a microcontroller with PID control logic. The non-inverting buck-boost converter circuit in this study is shown in Figures 5 and 6, which includes the schematic for the Arduino control circuit with voltage and current sensors. The selection of the trial and error method on PID control parameters with Kp = 0.8, Ki = 0.04, and Kd = 0.002 is because the designed system has nonlinear and dynamic characteristics, namely the energy source comes from a fluctuating pico-hydro cross flow turbine and solar panels, the load and environmental conditions change, and the mathematical model of the system is difficult to obtain precisely.

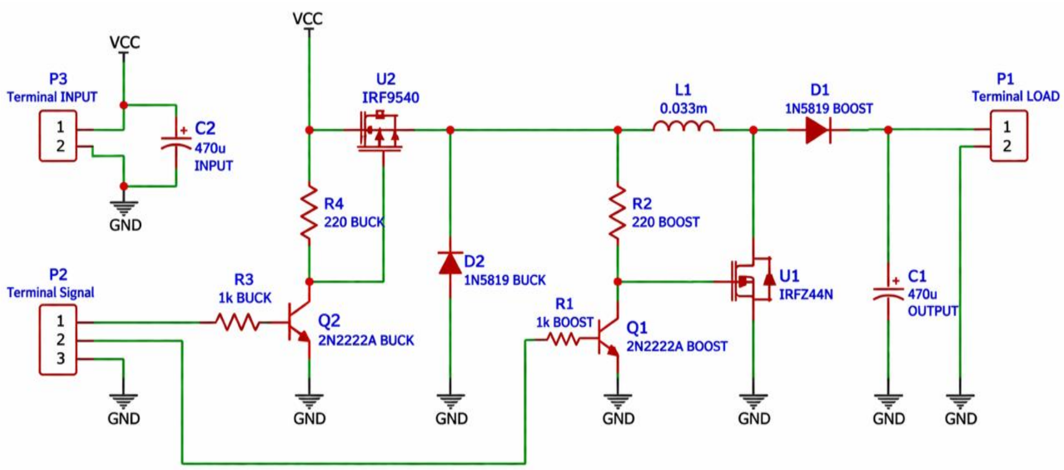

Figure 5. Network systems charging non-inverting buck-boost converter

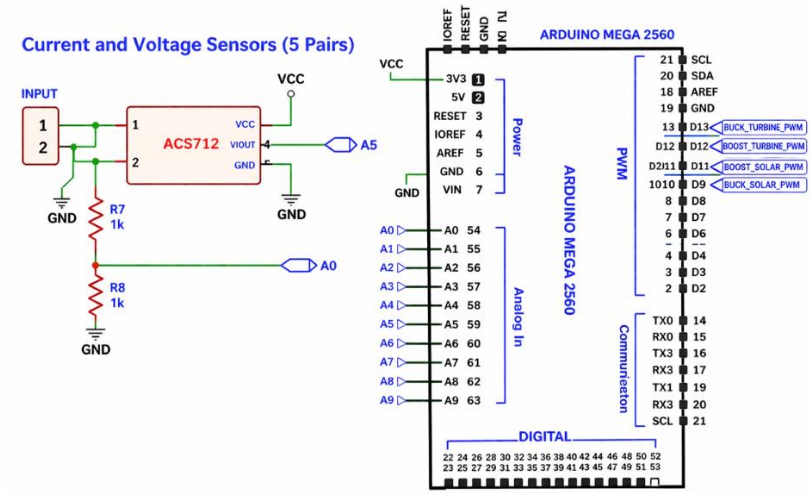

Figure 6. Arduino control series mega2560

3. RESULTS AND DISCUSSION

3.1. System design results

The design of the charging system for a hybrid power plant combining hydropower and solar panels was carried out with the assistance of additional software to ensure optimal design. After the design process was completed, the system was assembled according to the procedures described above. Thus, the final result of the charging system design for this hybrid power plant can be seen in Figure 7, which shows the implementation and final configuration of the designed system.

3.2. Solar panel testing

This test uses a solar panel with a capacity of 50 WP, which has the specifications as listed in Table 1. These specifications include technical parameters such as maximum voltage (Vmp), maximum current (Imp), no-load voltage (Voc), short-circuit current (Isc), as well as panel efficiency. Understanding these specifications is important to know the optimal working limits of the solar panels being tested.

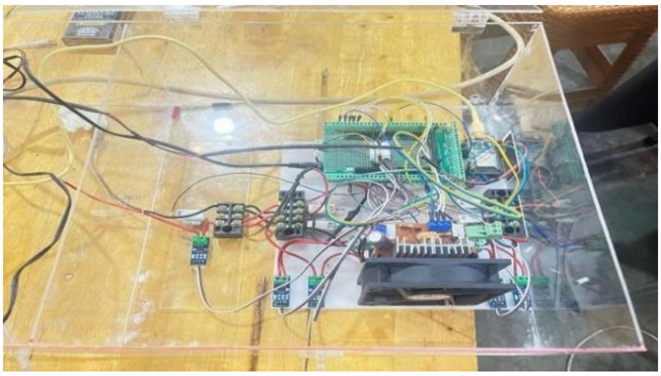

Figure 7. System design

Table 1. Specification of monocrystalline solar panel 50 WP

Specification of solar panel	Value
Maximum power (Pmax)	50 W
Voltage and Pmax (Vmp)	18.1 V
Current at Pmax (Imp)	2.78 A
Open circuit voltage (Voc)	22.2 V
Short circuit current (Isc)	2.96 A
Maximum system voltage	1000 VDC
Power tolerance	±3%

The test was carried out under two different conditions, namely without load and with load. In no-load conditions, measurements are made to determine the maximum voltage that solar panels can generate under certain conditions. Meanwhile, load testing is carried out by connecting solar panels to an electrical system to analyse how the voltage and electrical current generated can be used to power devices or supply power to energy storage systems.

3.2.1. Without load

In without load conditions, measurements are taken to determine the maximum voltage that solar panels can generate under various lighting conditions. This measurement aims to understand the output characteristics of the solar panel voltage in the absence of current flowing to the load. The test results under these conditions can be seen in Table 2, which shows the variation in the output voltage generated by the solar panel based on the intensity of light received at each hour of measurement. By knowing the value of the no-load voltage (Voc) under various conditions, it is possible to determine the maximum potential that the solar panel has before it is loaded. This data is a reference in analysing the performance of solar panels when used in the actual electrical system.

Table 2. Solar panels without load

Testing time	Light intensity (lux)	Surface temperature of solar panel (°C)	Voltage (V)
08.00	33740	31.4	20.6
09.00	61450	41.8	20.6
10.00	117200	38.5	21.0
11.00	146200	43.0	21.0
12.00	79700	44.3	20.8
13.00	75830	41.5	20.7
14.00	61070	41.2	20.6
15.00	47910	38.7	20.5
16.00	29740	34.7	20.3
17.00	22390	34.0	20.0

3.2.2. With load

The load used in this test is a lime resistor with a power of 20 watts and a resistance of 10 ohms. The selection of lime resistors as a load aims to provide a fixed load that allows the analysis of the current and voltage characteristics generated by the solar panel under real conditions. In this test, data is recorded every hour to obtain information about the voltage and electric current generated by the solar panel when connected to the load. Under load, the solar panel's output voltage will decrease compared to the no-load condition, so it's important to know the extent to which these changes occur. The data can be seen in Table 3.

Table 3. Solar panels with load

Testing time	Light intensity (lux)	Surface temperature of solar panel (°C)	Voltage (V)	Current (A)
08.00	33740	31.4	7.6	0.77
09.00	61450	41.8	12.8	1.30
10.00	117200	38.5	17.9	1.81
11.00	146200	43.0	18.7	1.87
12.00	79700	44.3	15.2	1.44
13.00	75830	41.5	14.7	1.39
14.00	61070	41.2	12.6	1.18
15.00	47910	38.7	10.2	0.96
16.00	29740	34.7	6.4	0.61
17.00	22390	34.0	4.8	0.46

Based on Tables 2 and 3, the increase in light intensity is directly proportional to the increase in the output voltage of the solar panel. In this test, when the light intensity reached a maximum value of 146200 lux at 11.00 WIB, the output voltage without load was recorded at 21.0 V, while with load it dropped to 18.7 V with a current of 1.87 A. On the other hand, when the light intensity is at its lowest point, which is 22390 lux at 17.00 WIB, the output voltage without load is 20.0 V and drops to 4.8 V when loaded with a current value of 0.46 A. So that the graph between the no-load voltage, the charged voltage, and the light intensity can be seen in Figure 8. The higher the intensity of the light received, the greater the voltage and current that solar panels can generate. This shows that the light intensity factor greatly affects the performance of solar panels in producing optimal electrical power.

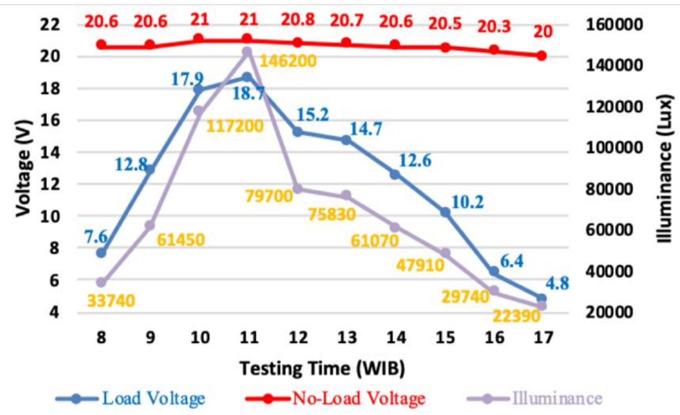

Figure 8. Graph of relationship without load voltage, with load voltage and light intensity

3.3. Crossflow water turbine testing

The test of this crossflow water turbine aims to analyse its performance characteristics in more depth. The testing process includes a variety of important parameters, such as the variation of the vane guide, the variation of the nozzle angle, the revolutions per minute (RPM) of the generator, as well as the output voltage generated during operation. Data collection is carried out systematically by considering two main conditions, namely, without load and with load. Testing under no load aims to determine the basic characteristics of turbines and generators while operating without external resistance, while testing under load aims to evaluate the performance of the system when generating power for a particular device or electrical system.

3.3.1. Without load

In without load conditions, crossflow turbine testing is carried out to analyze its performance without external obstacles. The test results are summarised in Figures 9 and 10, including the variation of the guide vane, nozzle angle, generator RPM, and output voltage produced. This data is used to understand the influence of parameters on turbine rotation and system efficiency before loading.

3.3.2. With load

The load used in this test is a 20-watt, 10 ohm lime resistor, which functions as an electrical load to simulate actual operational conditions. In this test, the parameters observed include the RPM of the generator, as well as the output voltage and current generated when the system is working with loads. Compared to no-load conditions, the results of these tests can provide an idea of how the load affects the turbine efficiency as well as the electrical power that the system can generate. In the test without load and with a load on the crossflow turbine, a graph of the relationship between the vane guide, nozzle angle, and voltage, as well as the generator RPM and output voltage produced by the generator, can be seen in Figures 11 and 12.

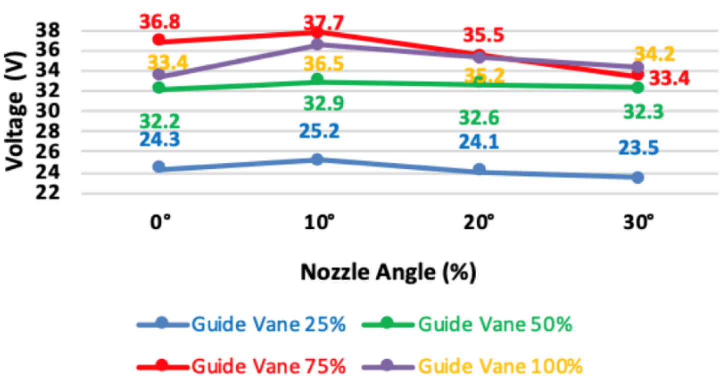

Figure 9. Voltage of the guide vane and nozzle angle without a load condition

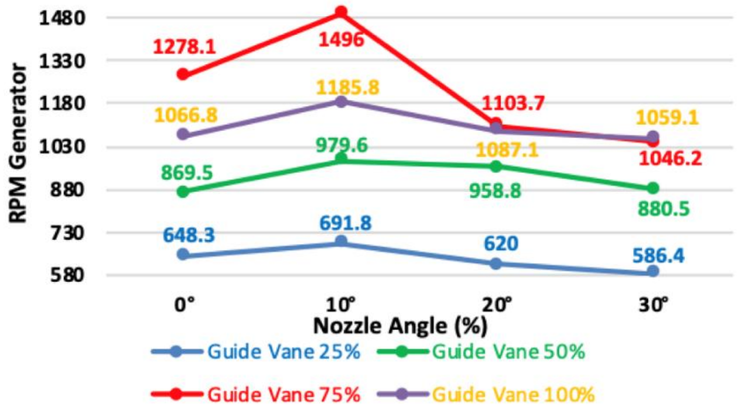

Figure 10. RPM of the guide vane and nozzle angle without a load condition

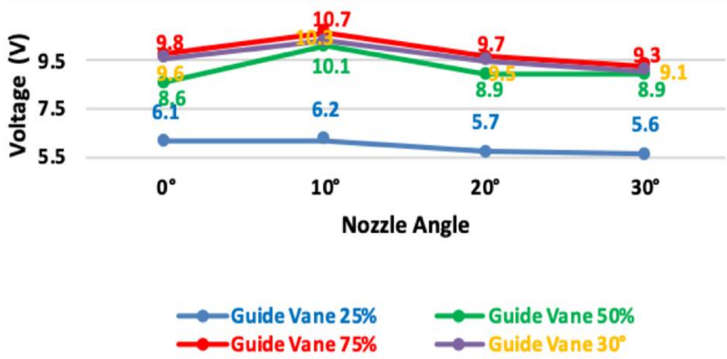

Figure 11. Voltage of the guide vane and nozzle angle with a load condition

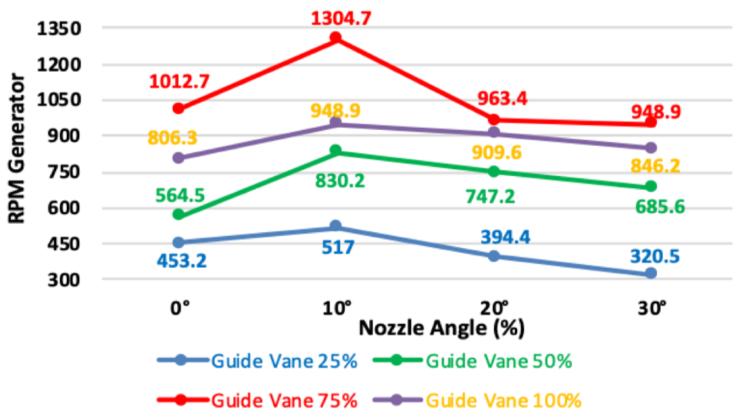

Figure 12. RPM of the guide vane and nozzle angle with a load condition

Based on the test results, it was concluded that the maximum voltage occurred when the generator RPM reached the highest value, with a 75% variation of the guide vane with a nozzle angle of 10°. In comparison, the minimum voltage occurred when the RPM of the generator was at the lowest value, with a variation of the guide vane of 25% with a nozzle angle of 30°. The data collected show the linear relationship between the generator's RPM and the output voltage of the generator. The higher the RPM produced, the greater the voltage generated by the generator. This indicates that RPM has a significant influence on the performance of generators in crossflow air turbines in producing electrical power optimally.

3.4. Testing buck-boost converter

In this test, a system design test was carried out on one of the types of buck-boost converters used in this study, namely the non-inverting buck-boost converter. This test aims to evaluate the performance of the non-inverting buck-boost converter. Data collection is carried out with the help of an adjustable power supply with various voltage values to analyse the performance of the non-inverting buck-boost converter under various operational conditions.

3.4.1. Buck mode

In the buck mode test, it is expected that the non-inverting buck-boost converter system that has been designed will be able to lower the voltage to a setpoint of 14.4 V. The test results data can be seen in Table 4. Furthermore, the error value generated by the system can be calculated using (1), and the duty cycle value can be determined through (2). Where D denotes the duty cycle (%), V_{out} denotes the output voltage, and V_{in} indicates the input voltage. In Table 4, data on buck mode performance in a system designed to maintain the desired setpoint value are obtained. In this mode, the system manages to lower the input voltage value greater than 14.4 V to the set value, with an error value of no more than 2%.

$$Error = \frac{V_{setpoint} - V_{ouput}}{V_{setpoint}} \times 100\% \quad (1)$$

$$D = \frac{V_{out}}{V_{in}} \quad (2)$$

3.4.2. Boost mode

In the boost mode test, it is expected that the non-inverting buck-boost converter system that has been designed will be able to lower the voltage to a setpoint of 14.4 V. The test results data can be seen in Table 5. The data on the performance of the boost mode on the system is obtained, which is designed to maintain the desired setpoint value.

Table 4. Test testing data buck

Vinput (V)	Voutput (V)	Duty cycle (%)	Error (%)
16	14.42	92	0.138
16.7	14.5	86.2	0.694
17	14.34	84.7	0.416
18	14.5	80	0.694
18.6	14.58	77.4	1.25
19.3	14.5	75.1	0.694
19.7	14.5	73.6	0.694
20	14.34	71.7	0.416
20.5	14.42	70.3	0.138
22	14.66	66.6	1.806

Table 5. Test testing data boost

Vinput (V)	Voutput (V)	Duty cycle (%)	Error (%)
8.1	14.5	44.1	0.694
8.5	14.42	41	0.138
9.2	14.66	34.5	1.806
9.6	14.5	33.7	0.694
10.2	14.34	28.8	0.416
10.8	14.5	25.5	0.694
11.1	14.5	24.1	0.694
12	14.42	17.9	0.138
12.6	14.58	13.9	1.25
13	14.42	11	0.139

3.5. Non-inverting buck-boost converter with PID control logic

At this stage of testing, a system design test was carried out on the non-inverting buck-boost converter with the addition of PID control logic. In addition, PID control parameters were also determined to be applied to the non-inverting buck-boost converter system for solar panels and crossflow water turbines. The process of determining these parameters uses the trial-and-error method. With the variation of several fluctuating voltage inputs, it is found that the best parameter is when the values of Kp (0.8), Ki (0.04), and Kd (0.002) are used. That way, the system can work well by producing the desired setpoint value.

3.6. Overall charging system testing

At this stage, integration testing was carried out on the entire solar panel system and air crossflow turbine by applying a non-inverting buck-boost converter based on PID control logic. In this test, the input and output values of the system that has been integrated with the designed system will be seen. This test aims to evaluate the performance of the system during charging on a 12V, 5 Ah battery pack. In this design, a hybrid current can produce a value with a range of ±1 A. The battery is found that charging a current of 0.5 A takes ±10 hours, and for a current of 5 A, it takes ±30 minutes. So, the author can assume that this charging test will take ±3 hours to charge. Therefore, this test was carried out at 10.00 WIB – 13.00 WIB, considering that this time is the optimal point for the use of solar panels. Meanwhile, the results of the charging test data from the solar panel power plant can be seen in Table 6. Furthermore, data on the system designed on the crossflow air turbine can also be seen in Table 7.

So that each non-inverting buck-boost converter in each plant will produce a voltage value that has been set at a setpoint of 14.4 V. Then each output of the non-inverting buck-boost converter will be paralleled to get the output value of the designed system and will be connected to the battery. Furthermore, the estimated time to charge the battery is obtained. This data can be seen in Table 8. It can be seen that the battery voltage reaches the full point of 13.85 V with a time record of 3 hours, so a graph is obtained showing the time needed to charge a 12 V, 5 Ah battery.

Table 6. Test testing data buck

Time	V input (V)	I input (A)	Vout buck-boost converter (V)	Iout buck-boost converter (A)	Error (%)
10.00	17.14	1.73	13.57	1.01	5.76
10.20	17.20	1.74	14.00	1.33	2.43
10.40	17.16	1.73	13.50	1.27	2.78
11.00	18.60	1.87	14.01	1.34	2.70
11.20	17.01	1.70	13.98	1.32	2.91
11.40	15.51	1.56	13.78	1.29	4.30
12.00	15.60	1.57	13.88	1.31	3.61
12.20	15.31	1.53	13.61	1.28	5.48
12.40	14.98	1.50	13.65	1.28	5.20
13.00	14.95	1.49	13.80	1.30	4.16

Table 7. Data hybrid from water turbine plants crossflow

Time	V input (V)	I input (A)	Vout buck-boost converter (V)	Iout buck-boost converter (A)	Error (%)
10.00	9.70	0.93	14.01	1.33	2.71
10.20	9.81	0.94	13.98	1.32	2.92
10.40	10.04	0.97	14.01	1.31	2.71
11.00	9.50	0.91	13.78	1.30	4.31
11.20	10.57	1.1	14.34	1.36	0.42
11.40	10.62	1.03	14.42	1.37	0.14
12.00	10.30	1.02	14.03	1.32	2.57
12.20	10.38	1.03	14.01	1.29	2.71
12.40	9.70	0.94	14.03	1.28	2.57
13.00	8.90	0.86	13.62	1.01	5.42

Table 8. System-wide integration data

Time	Solar panels		Water turbine		Hybrid		Error (%)	Battery voltage (V)
	V output (V)	I output (A)	V output (V)	I output (A)	V output (V)	I output (A)		
10.00	13.57	1.01	14.01	1.33	14.50	1.50	0.69	12.50
10.20	14.00	1.33	13.98	1.32	14.05	1.06	2.43	12.99
10.40	13.50	1.27	14.01	1.31	14.32	0.93	0.56	13.14
11.00	14.01	1.34	13.78	1.30	14.18	0.82	1.53	13.24
11.20	13.98	1.32	14.34	1.36	14.51	0.72	0.76	13.37
11.40	13.78	1.29	14.42	1.37	14.36	0.60	0.28	13.50
12.00	13.88	1.31	14.03	1.32	14.21	0.52	1.32	13.59
12.20	13.61	1.28	14.01	1.29	14.04	0.46	2.50	13.67
12.40	13.65	1.28	14.03	1.28	14.22	0.42	1.25	13.76
13.00	13.80	1.30	13.62	1.01	14.24	0.37	1.11	13.85

3.7. Testing discharging

Before discharging is carried out, the battery is first charged until it reaches full capacity. After that, the battery is connected to a load in the form of a 12 V, 30 W DC lamp to observe the duration of discharge until the battery reaches the minimum operating voltage. Keep in mind that discharging the battery does not completely discharge the battery, only to the voltage level of ±12.4 V. The data from these test results is then presented in Figure 13, which shows the time it takes, with a range of 5 minutes, until the battery is fully discharged. As shown in Figure 13, the discharging process takes 55 minutes to reach a voltage of 12.37 V. The graph shows the change in battery voltage during the discharging process over 5 minutes. This result also aligns with previous research, showing that the presence of PID leads to smaller errors [27]-[29].

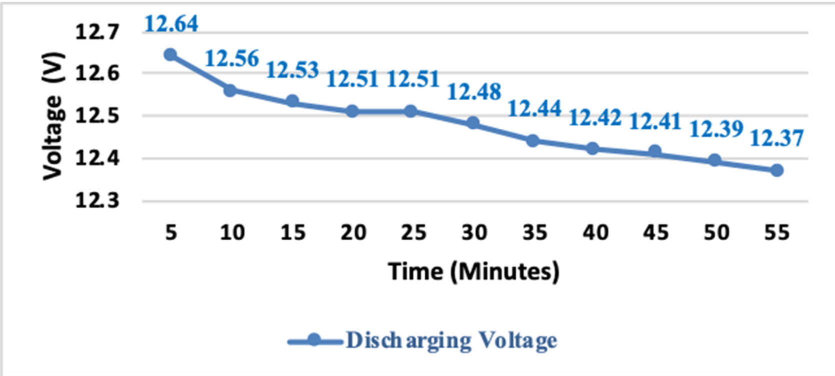

Figure 13. Graphs discharging battery

4. CONCLUSION

The use of a non-inverting buck-boost converter with PID control logic is crucial for maintaining the stability of the battery charging system. This converter maintains optimal voltage, preventing overvoltage and undervoltage. With a hybrid output, it can reach a setpoint of 14.4 V, with an average voltage of 14.263 V and an average error of 1.243%. Then, the experimental results demonstrate that integrating a non-inverting buck-boost converter with PID control provides robust voltage regulation during battery charging, maintaining a precise 14.4 V setpoint with minimal deviation and achieving full capacity within three hours, as specified by the manufacturer. In hydro power applications, optimisation of the cross-flow turbine's guide vane (75%) and nozzle angle (10°) significantly enhances energy conversion efficiency, producing 11.663 W of electrical output. For photovoltaic systems, light intensity is a dominant factor, with peak performance of 34.96 W at 146,200 lux and a substantial decline under reduced illumination. Collectively, these findings emphasise the critical interplay among advanced control strategies, mechanical optimization, and environmental parameters to maximise the efficiency and reliability of hybrid renewable energy systems. Future research may explore the implementation of alternative converter topologies, such as bidirectional DC–DC converters, to further enhance system efficiency. Additionally, employing more advanced battery discharging measurement systems is recommended to improve data accuracy. The PID control parameters in this study were determined through a trial-and-error approach, which may not yield optimal performance; therefore, future studies should consider systematic tuning methods, such as the Ziegler–Nichols technique or other optimization algorithms, to achieve superior control precision.

ACKNOWLEDGMENTS

Authors would like to express our highest gratitude to Universitas Sumatera Utara for supporting this research.

FUNDING INFORMATION

Authors state no funding involved.

AUTHOR CONTRIBUTIONS STATEMENT

This journal uses the Contributor Roles Taxonomy (CRediT) to recognize individual author contributions, reduce authorship disputes, and facilitate collaboration.

Name of Author	C	M	So	Va	Fo	I	R	D	O	E	Vi	Su	P	Fu
Yulianta Siregar	✓	✓	✓	✓	✓	✓		✓	✓	✓			✓	✓
Christian Kevin		✓				✓		✓	✓	✓	✓	✓		
Imanuel Simarmata														
Issarachai Ngamroo	✓		✓	✓			✓			✓	✓		✓	

C : **C**onceptualization
M : **M**ethodology
So : **So**ftware
Va : **Va**lidation
Fo : **Fo**rmal analysis
I : **I**nvestigation
R : **R**esources
D : **D**ata Curation
O : Writing - **O**riginal Draft
E : Writing - Review & **E**diting
Vi : **Vi**sualization
Su : **Su**pervision
P : **P**roject administration
Fu : **Fu**nding acquisition

CONFLICT OF INTEREST STATEMENT

Authors state no conflict of interest.

DATA AVAILABILITY

Derived data supporting the findings of this study are available from the corresponding author, [YS], on request.

REFERENCES

[1] M. N. Nasir and K. S. Bengi, “The energy mix dilemma in Indonesia in achieving net zero emissions by 2060,” *ASEAN Natural Disaster Mitigation and Education Journal*, vol. 2, no. 1, Jul. 2024, doi: 10.61511/andmej.v2i1.2024.951.

[2] K. Handayani and P. Anugrah, “Assessing the implications of net-zero emissions pathways: an analysis of the Indonesian power sector,” in *2021 International Conference on Technology and Policy in Energy and Electric Power (ICT-PEP)*, IEEE, Sep. 2021, pp. 270–275, doi: 10.1109/ICT-PEP53949.2021.9600954.

[3] A. Martalia, B. R. Saragih, and I. E. Sihombing, “The legal construction of new and renewable energy in Indonesia towards net zero emissions: a normative study on the policy development and utilisation of renewable energy in New Zealand,” *Law and Humanities Quarterly Reviews*, vol. 3, no. 3, Sep. 2024, doi: 10.31014/aior.1996.03.03.125.

[4] H. H. H. Mousa, A.-R. Youssef, and E. E. M. Mohamed, “State of the art perturb and observe MPPT algorithms based wind energy conversion systems: a technology review,” *International Journal of Electrical Power & Energy Systems*, vol. 126, p. 106598, Mar. 2021, doi: 10.1016/j.ijepes.2020.106598.

[5] T. A. Srinivas, M. J. S. Mohamed, S. A, P. Sukania, A. Pathani, and K. Sekar, “Smart highway technique using wind turbine with vertical axis (VAWT),” in *2022 International Conference on Power, Energy, Control and Transmission Systems (ICPECTS)*, IEEE, Dec. 2022, pp. 1–5, doi: 10.1109/ICPECTS56089.2022.10047666.

[6] C. Emeghara, P. I. Obi, O. A. John, and O. Emeghara, “Modeling and performance evaluation of a hybrid solar-wind power generation plant,” *Journal of Energy Technology and Environment*, vol. 4, no. 1, pp. 2022–2043, 2022.

[7] S. A. Shezan *et al.*, “Optimization and control of solar-wind islanded hybrid microgrid by using heuristic and deterministic optimization algorithms and fuzzy logic controller,” *Energy Reports*, vol. 10, pp. 3272–3288, Nov. 2023, doi: 10.1016/j.egyr.2023.10.016.

[8] R. Núñez and M. Victoria, “Solar radiation,” in *Fundamentals of Solar Cells and Photovoltaic Systems Engineering*, Elsevier, 2025, pp. 25–57, doi: 10.1016/B978-0-323-96105-9.00002-1.

[9] D. Sherman, J. Marquez, Y. Ramirez, M. Urbina, A. Meza, and D. Hodges, “Monocrystalline silicon solar cell simulation with reduced absorber thickness and efficiency exceeding 25%,” in *2021 IEEE 48th Photovoltaic Specialists Conference (PVSC)*, IEEE, Jun. 2021, pp. 2640–2642, doi: 10.1109/PVSC43889.2021.9518818.

[10] S. Praptodiyono, H. Maghfiroh, M. Nizam, C. Hermanu, and A. Wibowo, “Design and prototyping of electronic load controller for pico hydropower system,” *Jurnal Ilmiah Teknik Elektro Komputer dan Informatika*, vol. 7, no. 3, p. 461, Dec. 2021, doi: 10.26555/jiteki.v7i3.22271.

[11] S. W. L. Tobing, Z. Pane, and Y. Siregar, “Optimization of hydro turbine governor in a stand-alone hydro plant using PID control,” in *2021 5th International Conference on Electrical, Telecommunication and Computer Engineering (ELTICOM)*, IEEE, Sep. 2021, pp. 140–145, doi: 10.1109/ELTICOM53303.2021.9590115.

[12] R.-A. C. O. Calimpusan, L. P. Arcite, and J. M. A. Yula, “Design and enhancement of pico hydro and monitoring system for generation of electricity,” *International Journal of Engineering Trends and Technology*, vol. 72, no. 3, pp. 49–54, Mar. 2024, doi: 10.14445/22315381/IJETT-V72I3P105.

[13] Zulfikar, “Study of dynamic stability analysis in the Sigura-Gura hydro power plant using the power stabilizer system as compensation,” *IOP Conference Series: Materials Science and Engineering*, vol. 854, no. 1, p. 012065, May 2020, doi: 10.1088/1757-899X/854/1/012065.

[14] A. Ahmadi *et al.*, “Applications of geothermal organic Rankine Cycle for electricity production,” *Journal of Cleaner Production*, vol. 274, p. 122950, Nov. 2020, doi: 10.1016/j.jclepro.2020.122950.

[15] Y. Siregar, F. H. Siregar, E. Sinulingga, and Suherman, “Design of geothermal and solar hybrid renewable energy in Sipoholon Village, North Tapanuli Regency, North Sumatera,” in *2021 5th International Conference on Electrical, Telecommunication and Computer Engineering (ELTICOM)*, IEEE, Sep. 2021, pp. 60–63, doi: 10.1109/ELTICOM53303.2021.9590173.

[16] S. Ounnabi and H. Mounir, “Recent development of hybrid renewable energy systems,” in *2021 9th International Renewable and Sustainable Energy Conference (IRSEC)*, IEEE, Nov. 2021, pp. 1–7, doi: 10.1109/IRSEC53969.2021.9741165.

[17] S. A. G. Pinilih and W. L. Chairunnisa, “New and renewable energy policy in developing Indonesia’s National Energy Resilience,” *E3S Web of Conferences*, vol. 125, p. 10004, Oct. 2019, doi: 10.1051/e3sconf/201912510004.

[18] Aminuddin, B. Pranoto, M. I. A. Irsyad, A. L. Sihombing, and V. Nurliyanti, "Hybrid floating photovoltaic - hydropower potential utilization in Indonesia," *IOP Conference Series: Earth and Environmental Science*, vol. 1105, no. 1, p. 012004, Dec. 2022, doi: 10.1088/1755-1315/1105/1/012004.

[19] J. Koko, A. Riza, and U. K. Mohamad Khadik, "Design of solar power plants with hybrid systems," *IOP Conference Series: Materials Science and Engineering*, vol. 1125, no. 1, p. 012074, May 2021, doi: 10.1088/1757-899X/1125/1/012074.

[20] Y. Siregar, M. K. S. Tial, Y. F. S. Purba, S. Suherman, and S. Soeharwinto, "Design of solar cell using mirror, cooling, double axis, and solar tracking," *Indonesian Journal of Electrical Engineering and Computer Science*, vol. 28, no. 3, pp. 1297–1308, Dec. 2022, doi: 10.11591/ijeecs.v28.i3.pp1297-1308.

[21] Y. Siregar and Annisa, "Optimizing the design of the solar cell roof at Universitas Sumatra Utara by PVsyst," in *2022 6th International Conference on Electrical, Telecommunication and Computer Engineering (ELTICOM)*, IEEE, Nov. 2022, pp. 238–241, doi: 10.1109/ELTICOM57747.2022.10038259.

[22] A. V. Rao and G. K.P., "Analysis, design and simulation of non-inverting buck-boost DC-DC converter for battery charging," in *2021 International Conference on Disruptive Technologies for Multi-Disciplinary Research and Applications (CENTCON)*, IEEE, Nov. 2021, pp. 79–84, doi: 10.1109/CENTCON52345.2021.9688165.

[23] S. N. Soheli, G. Sarowar, M. A. Hoque, and M. S. Hasan, "Design and analysis of a DC-DC buck boost converter to achieve high efficiency and low voltage gain by using buck boost topology into buck topology," in *2018 International Conference on Advancement in Electrical and Electronic Engineering (ICAEEE)*, Nov. 2018, pp. 1–4, doi: 10.1109/ICAEEE.2018.8643001.

[24] K. A. Ogudo and P. Umenne, "Design of a PV based power supply with a noninverting buck-boost converter," in *2019 IEEE PES/IAS PowerAfrica*, IEEE, Aug. 2019, pp. 545–549, doi: 10.1109/PowerAfrica.2019.8928656.

[25] L. Larbi, S. Hadji, A. Belkaid, I. Colak, and R. Bayindir, "Design of a buck converter battery charging controller in PV plant," in *2022 10th International Conference on Smart Grid (icSmartGrid)*, IEEE, Jun. 2022, pp. 214–220, doi: 10.1109/icSmartGrid55722.2022.9848640.

[26] S. A. Kumar, M. N. Suneetha, and C. Lakshminarayana, "The simulation study of solar PV coupled synchronous buck converter with lead acid battery charging," in *2019 International Conference on Power Electronics Applications and Technology in Present Energy Scenario (PETPES)*, IEEE, Aug. 2019, pp. 1–4, doi: 10.1109/PETPES47060.2019.9003841.

[27] F. S. Dinniyah, W. Wahab, and M. Alif, "Simulation of buck-boost converter for solar panels using PID controller," *Energy Procedia*, vol. 115, pp. 102–113, Jun. 2017, doi: 10.1016/j.egypro.2017.05.011.

[28] N. F. Nanyan, M. A. Ahmad, and B. Hekimoğlu, "Optimal PID controller for the DC-DC buck converter using the improved sine cosine algorithm," *Results in Control and Optimization*, vol. 14, p. 100352, Mar. 2024, doi: 10.1016/j.rico.2023.100352.

[29] L. Ardhenta, M. R. Ansyari, R. K. Subroto, and R. N. Hasanah, "DC voltage regulator using buck-boost converter based PID-fuzzy control," in *2020 10th Electrical Power, Electronics, Communications, Controls and Informatics Seminar (EECCIS)*, IEEE, Aug. 2020, pp. 117–121, doi: 10.1109/EECCIS49483.2020.9263425.

BIOGRAPHIES OF AUTHORS

Yulianta Siregar did his undergraduate work at University of Sumatera Utara in Medan, North Sumatera Utara, Indonesia. He received a Bachelor of Engineering in 2004. After a while, he worked for a private company. He continued taking a master's program in electrical engineering at the Institute of Sepuluh Nopember, Surabaya, West Java, Indonesia, from 2007-2009. He was in a Ph.D. program at Kanazawa University, Japan, from 2016-2019. Until now, he has lectured at Universitas Sumatera Utara. He can be contacted at email: julianta_srg@usu.ac.id.

Christian Kevin Imanuel Simarmata is a fresh graduate of electrical engineering bachelor's degree from Universitas Sumatera Utara in 2025. Her research area of study is electrical power systems. He can be contacted at email: kevinsmart004@gmail.com.

Issarachai Ngamroo graduated from the Department of Electrical Engineering, School of Engineering, King Mongkut's Institute of Technology Ladkrabang (KMITL), Bangkok 10520, Thailand, in 1992. He received his M.Eng. and Ph.D. degrees from Osaka University, Japan, in 1997 and 2000, respectively. His research interests include power system stability, dynamics and controls, energy systems, renewable energy and energy storage applications, control, optimization, AI applications, network security, information security, and the internet of things. He is a professor of the Department of Electrical Engineering, School of Engineering, King Mongkut's Institute of Technology Ladkrabang (KMITL), Bangkok 10520, Thailand. He can be contacted at email: issarachai.ng@kmitl.ac.th.